SYNTHETIC BIOLOGY

Establishing a synthetic orthogonal replication system enables accelerated evolution in *E. coli*

Rongzhen Tian*, Fabian B. H. Rehm, Dariusz Czernecki, Yangqi Gu, Jérôme F. Zürcher, Kim C. Liu, Jason W. Chin*

The evolution of new function in living organisms is slow and fundamentally limited by their critical mutation rate. Here, we established a stable orthogonal replication system in *Escherichia coli.* The orthogonal replicon can carry diverse cargos of at least 16.5 kilobases and is not copied by host polymerases but is selectively copied by an orthogonal DNA polymerase (O-DNAP), which does not copy the genome. We designed mutant O-DNAPs that selectively increase the mutation rate of the orthogonal replicon by two to four orders of magnitude. We demonstrate the utility of our system for accelerated continuous evolution by evolving a 150-fold increase in resistance to tigecycline in 12 days. And, starting from a GFP variant, we evolved a 1000-fold increase in cellular fluorescence in 5 days.

The evolution of new function in living organisms is the result of continuous genomic mutation and selection within a population. This process is slow, and the rate of evolution is fundamentally limited by the critical mutation rate (*1*). Directed evolution commonly sidesteps the limitation on in vivo mutation rate by generating genetic diversity in vitro (*2*), but this does not enable the continuous evolution of genes within an organism. The mutation rate of cells can be transiently increased, but high levels of untargeted mutation lead to a catastrophic mutational load on the genome and are unsustainable. Genes inserted in viral genomes can be mutated by iteratively infecting new mutagenic cells (*3*–*6*). This approach sidesteps the challenge of increasing the rate of sustained mutation on genes in cells and can be extended to select for some phenotypes (*7*). However, this strategy is limited to evolving genes that are small enough to be packaged into viruses and to selecting phenotypes that can be coupled to infectivity; furthermore, selection occurs in cells under conditions of replicative stress, which may further limit the cellular phenotypes that can be explored.

Strategies that direct mutations to specific, targeted DNA sequences within cells without substantially increasing the genomic mutation rate offer the possibility of driving accelerated, sustainable, continuous, cellular evolution of target sequences (*8*–*17*). Pioneering work has taken advantage of an existing natural linear plasmid that functions in the yeast cytosol and is replicated by a dedicated, protein-primed DNA polymerase that does not copy the yeast genome as a natural orthogonal replication system (*12*, *13*). By recombining target genes into this existing linear plasmid system in yeast and generating mutagenic orthogonal DNA polymerases, a continuous evolution system was developed in this host. This system has been used to evolve metabolic pathways and antibodies and provided key insights into evolutionary trajectories (*12*, *13*, *18*). However, the system cannot be used for engineering bacterial genetic elements and requires additional steps to engineer the established replicons in vivo. Moreover, the doubling time of yeast makes this system theoretically slower than bacterial systems. Recent work has shown that target genes can also be recombined into a natural linear plasmid in *Bacillus thuringiensis*, and this system can also be used to generate a mutagenic orthogonal replication system (*14*). However, there are very limited genetic tools in this organism and the host is not widely used or well characterized.

Escherichia coli is the workhorse of molecular biology and is widely used in both fundamental discovery science and industrial production (*19*). It is the best characterized organism, and many of its biochemical pathways have been characterized in detail. It has a rapid doubling time (~20 min) and is a preferred host for gene cloning and protein expression, and a vast repertoire of genetic tools have been developed for this organism over many years. An outstanding challenge over the past decade has been to discover a stable orthogonal replication system that operates in *E. coli* and thereby enables accelerated continuous evolution in this host. However, despite substantial effort, no stable orthogonal replication system has been discovered in *E. coli*.

Results

Establishing a synthetic linear DNA replication system in vivo

PRD1 is a lytic phage that infects *E. coli*, undergoes uncontrolled replication, and lyses cells in 60 min (Fig. 1A and fig. S1) (*20*). Its linear, double-stranded genome encodes at least 25 gene products from five annotated operons under the control of eight annotated promoters and terminators (*21*). The ends of the linear genome are composed of inverted terminal repeats (ITRs) that form the binding site for the terminal protein (TP) and function as origins of replication (Fig. 1B) (*22*). The early operons contain the genes responsible for replication of the PRD1 genome. The left early operon encodes the TP and the DNA polymerase (DNAP), and the right early operon encodes phage single-stranded DNA binding protein (SSB) and double-stranded DNA-binding protein (DSB). The central operons contain the genes encoding the remaining structural and lytic protein components of PRD1.

To generate a synthetic system for the controlled replication of a linear replicon (Fig. 1A), we separated the four genes that we hypothesized might be essential for in vivo replication of the PRD1 genome from the structural and lytic genes and combined them into a single synthetic replication operon controlled by an isopropyl-β-D-thiogalactopyranoside (IPTG)–inducible promoter, PtacIPTG (Fig. 1B). We hypothesized that this synthetic replication operon might be sufficient to direct the replication of any linear double-stranded DNA flanked by PRD1 ITR sequences in *E. coli* without leading to the uncontrolled replication and cell lysis mediated by the parent phage. We integrated the synthetic replication operon into the genome of *E. coli* to create a strain primed for replicating a linear replicon composed of linear double-stranded DNA flanked by PRD1 ITR sequences.

We created a Kan^R-GFP linear replicon composed of a kanamycin resistance gene and a *GFP* gene under the control of constitutive promoters flanked by 110-bp PRD1 ITR sequences on each end; the sequence was amplified by polymerase chain reaction (PCR) (Fig. 1C). We electroporated this replicon into *E. coli* bearing the synthetic replication operon in their genome and plated the cells on agar plates containing IPTG to express the operon and kanamycin to maintain the replicon. We obtained 9 ± 4 colonies per 100 μl of competent cells that grew on kanamycin and exhibited green fluorescent protein (GFP) fluorescence, which is consistent with the linear replicon being present in cells (Fig. 1D). We did not observe growth on kanamycin when the linear replicon was electroporated into cells that did not contain the synthetic replication operon, demonstrating that the synthetic replication operon is necessary for the maintenance of the linear replicon (Fig. 1D). Purification of the linear replicon and analysis by agarose gel electrophoresis confirmed the presence of the linear replicon in cells (Fig. 1E). Taken together, our experiments demonstrate that we have created a linear replicon that requires the synthetic replication operon for its maintenance and replication.

Medical Research Council Laboratory of Molecular Biology, Cambridge, UK.
*Corresponding author. Email: rtian@mrc-lmb.cam.ac.uk (R.T.); chin@mrc-lmb.cam.ac.uk (J.W.C.)

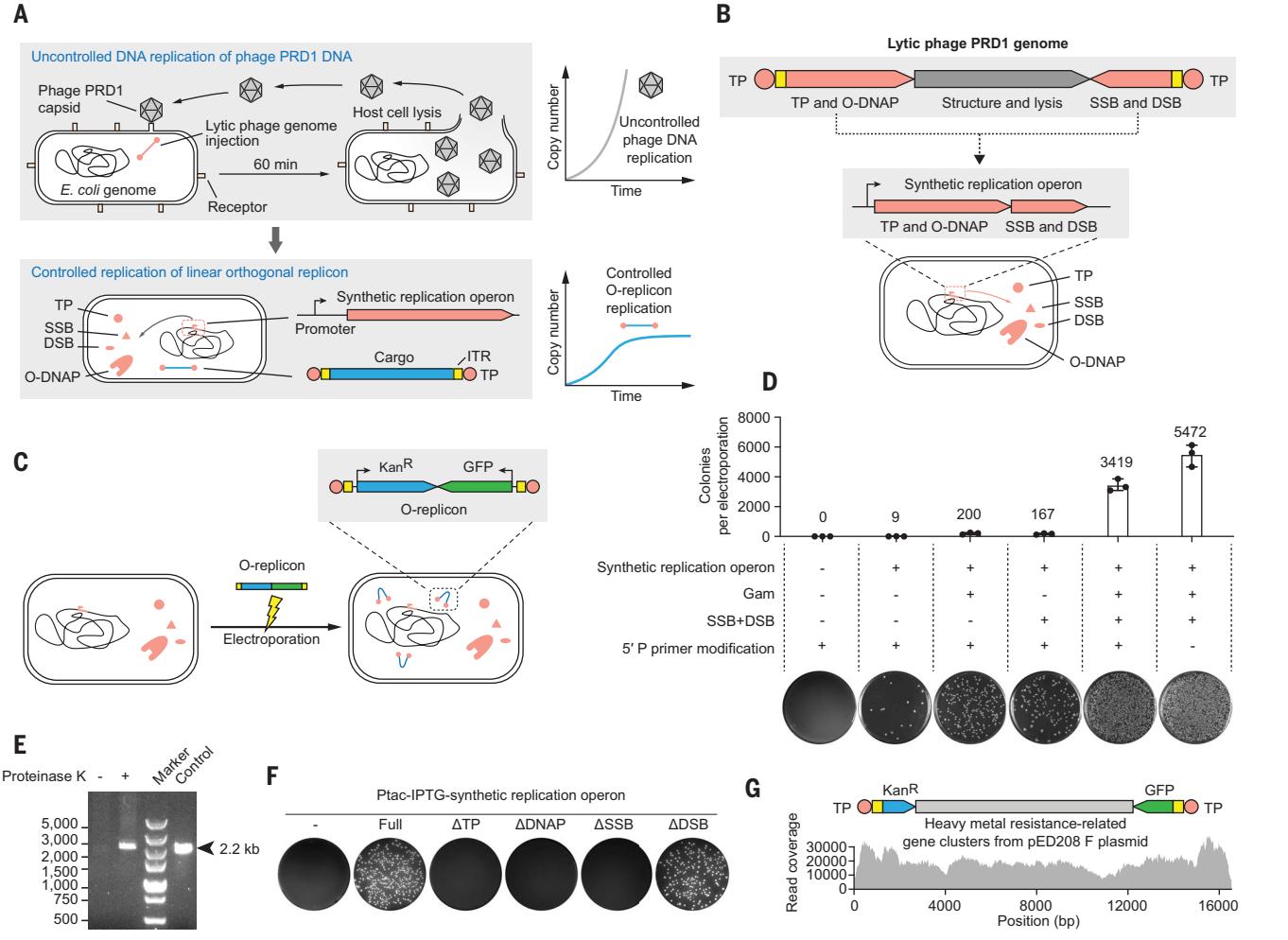

Fig. 1. Establishing a synthetic orthogonal replicon in *E. coli*. (**A**) PRD1 undergoes uncontrolled replication upon infecting *E. coli* and rapidly lyses host cells. Constructing a synthetic operon enables controlled replication of an orthogonal replicon. ITRs are shown in yellow. (**B**) We combined genes for replication of the orthogonal replicon to generate a synthetic replication operon. (**C**) Orthogonal replicons can be established by electroporating into *E. coli* cells harboring a genomic synthetic replication operon. The linear Kan^R-GFP replicon consists of flanking 110-bp ITR, a kanamycin resistance gene, and a GFP gene. (**D**) Efficiency of establishing orthogonal replicons by electroporating 3 μg of Kan^R-GFP PCR product into 100 μl (~10^9 cells). Expression of *gam*, *ssb*, and *dsb* genes from a helper plasmid increased efficiency (n = 3, error bars indicate ± SD). (**E**) Extraction of the Kan^R-GFP orthogonal replicon from cells. Proteinase K addition was needed to remove the terminal proteins. The control is a PCR product. (**F**) Essentiality of genes in the synthetic replication operon for establishing the orthogonal replicon. (**G**) A 16.5-kb orthogonal replicon. Shown is the Illumina sequencing read coverage.

We next sought to increase the efficiency with which the linear replicon could be established in cells. We expressed the Gam protein from the lambda phage, which inhibits host nucleases (RecBCD and SbcCD) and thereby protects linear double-stranded DNA from degradation (*23*), and found that it increased the number of colonies 22-fold. Overexpression of PRD1 *ssb* and *dsb* increased colony formation comparably to *gam* (Fig. 1D). Overexpressing *gam*, PRD1 *ssb* and *dsb* together increased the number of colonies 380-fold with respect to the original system. Switching to using non-phosphorylated primers with overexpressed *gam*, *ssb*, and *dsb* generated the most efficient transformation system and increased the number of colonies 608-fold with respect to the original system (Fig. 1D). The helper plasmids used to express *gam*, *ssb*, and *dsb*, were easily cured from cells once the linear replicon was established in cells (fig. S2).

We electroporated the Kan^R-GFP linear replicon into *E. coli* cells transformed with a single-copy plasmid bearing a synthetic replication operon in which one of each of the four genes in the operon (encoding TP, DNAP, SSB, and DSB) was disrupted (Fig. 1F). These experiments demonstrated that the DNAP, TP, and SSB, but not DSB, are necessary for establishing the linear replicon. Because the linear replicon is replicated by the PRD1-derived DNAP, but not the host DNAPs, we refer to it as an orthogonal replicon.

Using the most efficient transformation system, we established in vivo replication for a 16.5-kb orthogonal replicon (Fig. 1G). This demonstrates that we can use the system for large cargos.

Orthogonal replicon is stably inherited

To investigate the stability of the orthogonal replicon through many cell divisions, we followed the percentage of cells that maintain the Kan^R-GFP orthogonal replicon, as judged by the percentage of cells positive for GFP fluorescence shown by fluorescence-activated cell sorting (FACS), over 300 generations (Fig. 2A and fig. S3). In the presence of kanamycin, the Kan^R-GFP orthogonal replicon was stably maintained for 300 generations (Fig. 2A). In the absence of kanamycin, GFP fluorescence began to decay after ~50 generations (Fig. 2A). We obtained similar results using alternative

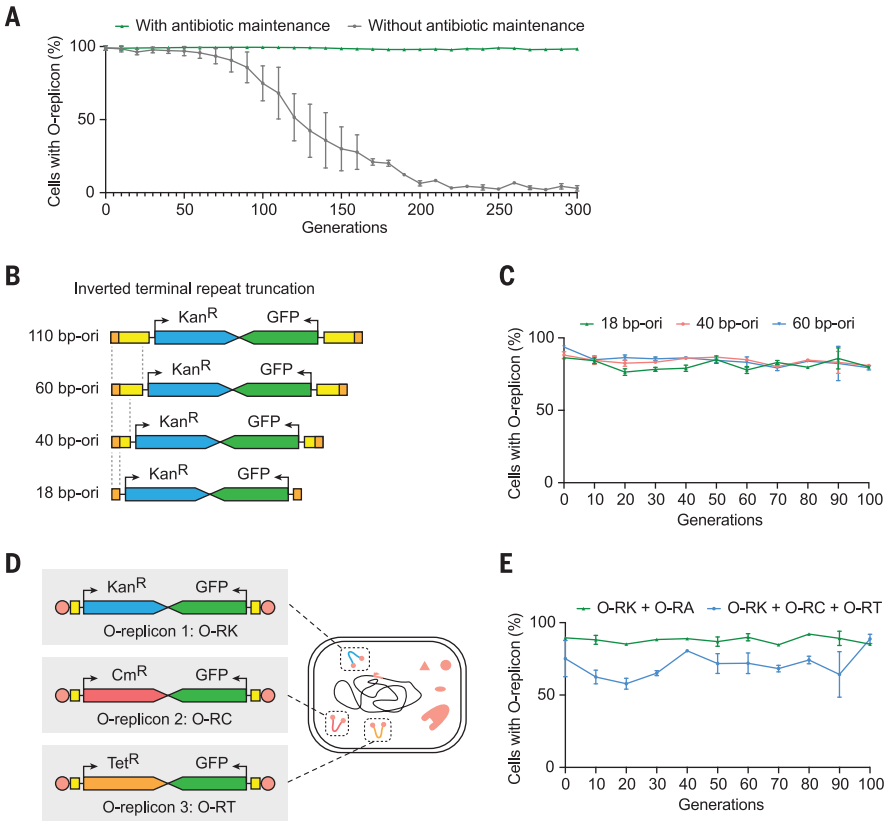

Fig. 2. Orthogonal replicons are stably maintained for hundreds of generations. (**A**) Stability of the Kan^R-GFP orthogonal replicon over 300 generations with or without kanamycin, as assessed by maintenance of GFP fluorescence using flow cytometry. The synthetic replication operon was under the control of a P*dnaKJ* promoter. (**B**) The ITR origins were iteratively truncated to establish a minimal origin for an orthogonal replicon. A single 18-bp repeat is shown in orange and the rest of the ITR in yellow. (**C**) Stability over 100 generations of the truncated orthogonal replicons shown in (B) in the presence of kanamycin as assessed by maintenance of GFP fluorescence using flow cytometry. (**D**) Multiple distinct orthogonal replicons were sequentially transformed and co-maintained under selection. (**E**) Stability, over 100 generations, of two or three co-maintained orthogonal replicons, as shown in (D), in the presence of the corresponding antibiotics as assessed by the maintenance of GFP fluorescence using flow cytometry. For the doubly transformed cells, O-RA corresponds to an orthogonal replicon carrying Amp^R. For all experiments, n = 3 and data are shown as mean ± SD.

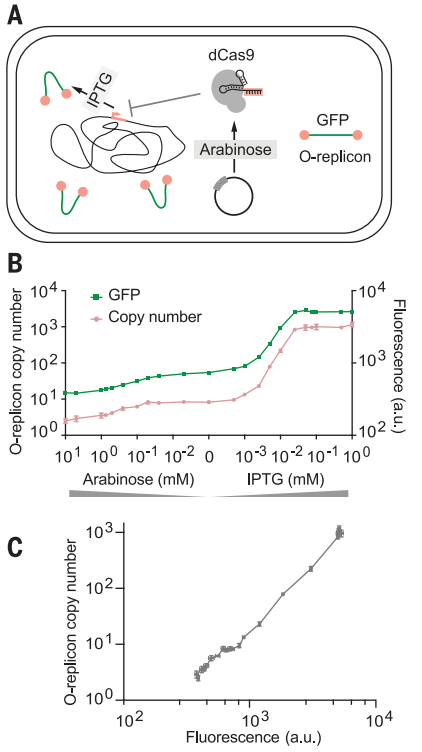

Fig. 3. Control of orthogonal replicon copy number over a 465-fold range. (**A**) Control of the orthogonal replicon copy number is achieved by inducing expression of the synthetic replication operon through IPTG addition or by down-regulating its expression using an arabinose-inducible dCas9 targeted to the IPTG-responsive Ptac promoter. (**B**) Orthogonal replicon copy number, as determined by quantitative PCR, and GFP fluorescence (normalized to OD_{600}) were measured at different arabinose or IPTG concentrations. (**C**) Correlation between Kan^R-GFP orthogonal replicon copy number and GFP fluorescence. Data from (B) were replotted for (C). For all experiments, n = 3 and data are shown as mean ± SD.

promoters to control the genomically integrated synthetic replication operon (fig. S3). These experiments demonstrated that the orthogonal replicon can be stably maintained in cells for many generations, as required for directed evolution using orthogonal replication systems.

Defining minimal origins of replication for the orthogonal replicon

To determine the minimal origin length required to establish an orthogonal replicon in cells, we prepared linear DNA with iteratively truncated ITRs (Fig. 2B). We found that replicons with ITRs truncated to 60, 40, or 18 bp could readily be established and maintained under selection for at least 100 generations (Fig. 2C and fig. S4). Linear DNA bearing 10 bp of the ITRs did not enable the replicon to be established, which is in agreement with an in vitro study of minimal PRD1 replication origins (*24*). Aligning the left origin of the PRD1 phage to the left origins of other *Tectiviridae* phages that prey on *E. coli* revealed that this minimal 18-bp sequence was conserved (fig. S1B).

Maintaining multiple distinct orthogonal replicons simultaneously

To test whether multiple distinct orthogonal replicons could be maintained in the same cell simultaneously, we sequentially established orthogonal replicons carrying different selection markers in cells (Fig. 2D). We found that at least three orthogonal replicons could be maintained simultaneously, under selection, for at least 100 generations (Fig. 2E). This may enable the directed evolution of multigene pathways without the requirement for these genes to be on a contiguous stretch of DNA.

Controlling orthogonal replicon copy number

Next, we modulated the copy number of an orthogonal replicon (expressing GFP from a constitutive promoter) in cells containing the IPTG-inducible synthetic replication operon (Fig. 3A and fig. S5). Cells also contained an arabinose-inducible dCas9 targeted to repress the IPTG-responsive Ptac promoter on the synthetic replication operon (fig. S6). By addition of arabinose or IPTG to cells, we modulated the copy number of the orthogonal replicon 466-fold, from 2.5 to 1166 copies per cell (Fig. 3B). We observed an increase in fluorescence resulting from GFP expression with increasing

orthogonal replicon copy number (Fig. 3C and fig. S7). In all cases, we further validated the precise orthogonal replicon copy numbers using quantitative PCR. These experiments demonstrated that we could regulate the copy number of the orthogonal replicon, and therefore gene expression from the orthogonal replicon, over a wide dynamic range.

Mutagenic DNA polymerases for the orthogonal replicon

To measure the mutation rate of the orthogonal replicon, we performed fluctuation analysis (*25*, *26*). We introduced a Kan^R-Cm^R(Q38TAG) orthogonal replicon that contains an amber stop codon (TAG) at position 38 of the chloramphenicol resistance gene (Cm^R) into cells containing a genomically encoded synthetic replication operon with a wild-type (WT) DNAP. We switched from using the genomically encoded WT DNAP to primarily using the plasmid-encoded DNAP of interest for replicating the orthogonal replicon by dCas9-meditated suppression of the genomically encoded synthetic replication operon and induction of plasmid encoded synthetic replication operons with mutagenic polymerases (fig. S8). After 10 generations, we measured the fraction of Cm-resistant cells resulting from point mutations that convert the TAG stop codon to sense codons. Because a single copy of the intact Cm^R gene is sufficient to confer chloramphenicol resistance, we also measured the copy number of the orthogonal replicon (fig. S9). We used this information to calculate the apparent genomic mutation rate [μ, in substitutions per base pair per generation (s.p.b.)] for the DNAP at the TAG codon in the orthogonal replicon (fig. S9). The apparent mutation rate for the WT DNAP was 8.96×10^{-10} s.p.b. We designed nine DNAPs (fig. S9) with the goal of increasing the mutation rate of the orthogonal replicon. The mutant DNAPs increased the apparent mutation rate to between 2.3×10^{-8} and 7.6×10^{-6} s.p.b. (fig. S9). The error rates of some of these DNAPs exceed the threshold of 4×10^{-7} s.p.b. that has previously been experimentally shown to lead to loss of viability with any further increase in mutagenesis (*27*). We focused on characterizing two mutant DNAPs, N71D and Y127A, because these mutant DNAPs supported linear orthogonal replicon copy numbers comparable to the WT DNAP (fig. S9). The mutation rate of the DNAPs N71D and Y127A were 9.13×10^{-7} and 5.61×10^{-7} s.p.b., respectively (Fig. 4).

O-DNA polymerases do not copy the genome

To measure the genomic mutation rate in cells containing each DNAP (WT, N71D, and Y127A), we introduced a Cm^R(Q38TAG) gene into the genome of strains containing the synthetic replication operon and switched from using the genomically encoded WT DNAP to primarily using the plasmid encoded DNAP of interest to copy the orthogonal replicon. After 10 generations, we measured the fraction of Cm-resistant cells resulting from point mutations that convert the TAG stop codon in the genome to sense codons and calculated the genomic mutation rate (μ) at the TAG codon. The genomic mutation rates with each mutant DNAP were indistinguishable from the genomic mutation rate in unmodified WT cells (Fig. 4). Moreover, the genomic mutation rates that we measured (6.4×10^{-10} s.p.b.) were comparable to those previously reported for *E. coli* (*28*, *29*). We conclude that the DNAP mutants can increase the mutation rate for replication of the orthogonal replicon without affecting the mutation rate of the genome, which is replicated by host DNAPs. The mutation rate for replication of the orthogonal replicon by the N71D and Y127A mutant DNAPs is approximately three orders of magnitude higher than the mutation rate of the genome. Overall, we conclude that the DNAP for the orthogonal replicon is an orthogonal DNAP (O-DNAP) and the orthogonal replicon and the synthetic replication operon (which contains the O-DNAP) constitute an *E. coli* orthogonal replication system (EcORep).

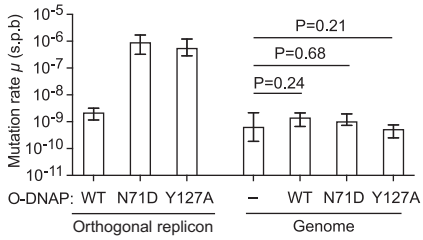

Fig. 4. Mutagenic orthogonal DNA polymerases selectively mutate the orthogonal replicon but not the genome. Determination of genomic or orthogonal replicon mutation rate (μ, in s.p.b.) for the O-DNAP and its engineered variants. The mutation rate was measured after 10 generations with fluctuation tests. For assessment of the orthogonal replicon mutation rate, we used an orthogonal replicon–encoded Cm^R gene with a TAG stop codon at position 38, and the O-DNAP variants were expressed from genomically integrated synthetic replication operons. For assessment of the genome mutation rate, we used a genomically encoded Cm^R gene with a TAG stop codon at position 38, and the O-DNAP variants were expressed from p15A plasmids using rhamnose induction. For all experiments, $n = 12$ and data are shown as mean ± upper or lower 95% bounds.

Accelerated continuous evolution of tigecycline resistance

Next, we investigated whether we could use the orthogonal replication system to continuously evolve new functions. We first investigated converting the tetracycline resistance gene *tetA* into a gene that confers resistance to tigecycline. We grew cells containing a Kan^R-TetA orthogonal replicon, which is primarily replicated by mutagenic (plasmid encoded) O-DNAPs in increasing concentrations of tigecycline (fig. S10). We completed 14 passages in 12 days. We performed 12 replicates with O-DNAP (N71D) and 12 replicates with O-DNAP (Y127A), with similar results.

After selection, we switched to replicating the orthogonal replicon with the WT O-DNAP so that it was not subject to further mutation. We obtained pools of cells that grew on 150 μg ml^{-1} tigecycline (Fig. 5A and fig. S11). For comparison, cells containing the WT *tetA* gene on the orthogonal replicon grew on agar plates containing tigecycline at 0.5 μg ml^{-1} but failed to grow on 2.5 μg ml^{-1} tigecycline. We identified numerous mutations across the promoter and 5′-untranslated region (5′-UTR), as well as synonymous and nonsynonymous mutations in the open reading frame (figs. S12 and S13 and data S1). Our experiment directly identifies mutations in *tetA* that have previously been implicated in tigecycline resistance, as well as a series of new mutations (Fig. 5B, data S1, and fig. S11). In contrast to previous work, we increased tolerance to both tigecycline and tetracycline simultaneously (fig. S11) (*10*).

We cloned selected genes into a standard circular plasmid (with a copy number ~5-fold lower than that of the orthogonal replicon). The evolved *tetA* genes conferred tigecycline resistance to 37 μg ml^{-1}, whereas the parent *tetA* gene conferred resistance to 0.25 μg ml^{-1}, and a previously reported *tetA* gene for tigecycline resistance conferred resistance to 0.5 μg ml^{-1} (Fig. 5C and fig. S14) (*10*). We conclude that in 12 days, we evolved tigecycline resistance genes that conferred resistance to 150 times more tigecycline than the starting gene and 74 times more tigecycline than in previous work.

Accelerated continuous evolution of GFP fluorescence

Next, we aimed to continuously evolve a *GFP* gene for increased green fluorescence. We grew cells containing a Kan^R-GFP orthogonal replicon in which "GFP" is a weakly fluorescing T66H variant of sfGFP (fig. S15) on a weak promoter; for simplicity, we refer to our starting variant as "WT GFP." The replicon was primarily replicated by (plasmid-encoded) mutagenic O-DNAPs (fig. S16).

To diversify the *GFP* gene and promoter, cells were diluted 1000-fold from a saturated culture and grown for 12 hours before 1000-fold dilution into fresh medium. This process was repeated four times over 48 hours before cells were sorted for GFP fluorescence. The resulting cells were then grown for a further 48 hours, with sorting for GFP fluorescence

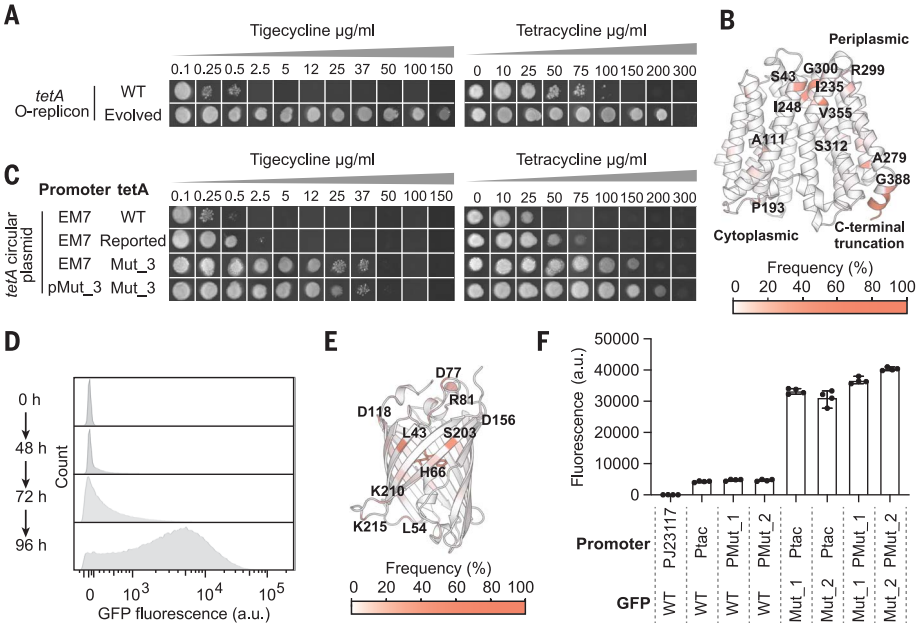

Fig. 5. Accelerated continuous evolution of tigecycline resistance and GFP fluorescence in cells. (**A**) Analysis of an evolved pool (after 14 passages) of cells carrying the Kan^R-TetA orthogonal replicon. Shown is the pool for replicate 10 performed with the N71D O-DNAP; fig. S13 shows other replicates. (**B**) AlphaFold2 model of TetA. Gradient indicates the mutational frequency of each residue. (**C**) Validation of evolved *tetA* on a ColE1 plasmid. Shown is Mut_3 from the replicate 10 pool; fig. S15 shows other mutants. Either the EM7 promoter or the evolved promoter (pMut_3) were used to drive expression. WT *tetA* or a previously reported mutant were assessed for comparison. (**D**) To select for brighter variants of a Kan^R-GFP orthogonal replicon, we iteratively isolated the brightest 0.1% of cells through FACS. Replicate 12 from the Y127A O-DNAP is shown; fig. S18 shows other replicates. (**E**) Structure of GFP (2B3P). Gradient indicates the mutational frequency of each residue. (**F**) Validation of evolved *GFP* and/or evolved promoter variants on a ColE1 plasmid. PMut_1 and Mut_1 were obtained with the N71D O-DNAP; PMut_2 and Mut_2 were obtained with the Y127A O-DNAP. For all experiments, n = 4 and data are shown as mean ± SD.

at 24 and 48 hours. All 12 replicates of this experiment for each of the two O-DNAPs were performed in <5 days (fig. S16). The population of cells progressively increased in fluorescence over the course of the experiment (Fig. 5D and fig. S17).

After selection, we switched to replicating the orthogonal replicon with the WT O-DNAP and reduced the copy number of the orthogonal replicon from 195.1 ± 3.4 and 300.5 ± 24.7 (for the N71D and Y127A O-DNAP mutants, respectively) to 9.1 ± 0.7 and 7.4 ± 0.2 (fig. S16). We then used FACS to identify clones with strong fluorescence.

Sequencing of selected clones identified numerous mutations across the promoter and 5′-UTR, as well as synonymous and nonsynonymous mutations in the open reading frame (Fig. 5E, figs. S18 and S19, and data S2). Our experiment directly identified mutations in the promoter that convert the –10 sequence to a consensus sequence and identified a number of enriched mutations in the coding sequence (fig. S19).

We picked colonies that exhibited strong fluorescence and cloned the corresponding gene into a standard circular plasmid. The selected constructs (pMut_1/GFP Mut_1 and pMut_2/GFP Mut_2) produced 36,586 ± 874 and 40,335 ± 442 arbitrary units (au) of fluorescence, respectively, whereas the starting WT *GFP* gene produced 33 ± 24 au of fluorescence (Fig. 5F and fig. S20). Thus, selection using the orthogonal replication system increased the cellular green fluorescence by >1000-fold in 5 days. Additional experiments demonstrated that mutations in both the promoter and the open reading frame of GFP make contributions to the observed increase in cellular fluorescence (Fig. 5F and figs. S21 and S22).

Discussion

We have established an orthogonal replicon in a living organism, *E. coli*, the most widely used and best characterized host, by endowing cells with a rationally designed synthetic replication operon. Our work demonstrates that orthogonal replication systems can be created de novo to enable the generation of mutagenic continuous cellular evolution systems in organisms beyond the extremely limited set in which natural replicons have been modified in vivo (*12*–*14*). The orthogonal linear double-stranded DNA replicon simply requires 18-bp DNA sequences at each end and can carry diverse cargos, including cargos too large for viral systems. The dynamic range of our control over replicon copy number exceeds that of control systems for circular plasmid copy number (*30*, *31*). Control over copy number allows control over evolutionary dynamics. Low copy number and stringent selection should favor the direct discovery of the desired genotypes that are proximal to the sequence of the starting gene. By contrast, high copy number may favor the exploration of more distal sequence space, thereby enabling the crossing of fitness valleys. These different evolutionary dynamics may be preferred in different circumstances.

EcORep provides a simple, stable, and scalable platform for accelerated continuous evolution in *E. coli*. We anticipate that it will substantially accelerate the development of diverse research tools, biopharmaceutical leads, and strains for the production of industrial chemicals.

REFERENCES AND NOTES

1. M. Lynch, *Trends Genet.* **26**, 345–352 (2010).
2. M. S. Packer, D. R. Liu, *Nat. Rev. Genet.* **16**, 379–394 (2015).
3. N. M. Low, P. H. Holliger, G. Winter, *J. Mol. Biol.* **260**, 359–368 (1996).
4. C. M. Berman *et al.*, *J. Am. Chem. Soc.* **140**, 18093–18103 (2018).
5. J. G. English *et al.*, *Cell* **178**, 748–761.e17 (2019).
6. C. E. Denes *et al.*, *ACS Synth. Biol.* **11**, 3544–3549 (2022).
7. K. M. Esvelt, J. C. Carlson, D. R. Liu, *Nature* **472**, 499–503 (2011).
8. C. L. Moore, L. J. Papa 3rd, M. D. Shoulders, *J. Am. Chem. Soc.* **140**, 11560–11564 (2018).
9. A. Cravens, O. K. Jamil, D. Kong, J. T. Sockolosky, C. D. Smolke, *Nat. Commun.* **12**, 1579 (2021).
10. X. Yi, J. Khey, R. J. Kazlauskas, M. Travisano, *Sci. Adv.* **7**, eabg8712 (2021).
11. S. O. Halperin *et al.*, *Nature* **560**, 248–252 (2018).
12. A. Ravikumar, G. A. Arzumanyan, M. K. A. Obadi, A. A. Javanpour, C. C. Liu, *Cell* **175**, 1946–1957.e13 (2018).
13. A. Ravikumar, A. Arrieta, C. C. Liu, *Nat. Chem. Biol.* **10**, 175–177 (2014).
14. R. Tian *et al.*, *Nat. Chem. Biol.* **19**, 1504–1512 (2023).
15. M. Camps, J. Naukkarinen, B. P. Johnson, L. A. Loeb, *Proc. Natl. Acad. Sci. U.S.A.* **100**, 9727–9732 (2003).
16. C. Fabret *et al.*, *Nucleic Acids Res.* **28**, E95 (2000).
17. G. T. Hess *et al.*, *Nat. Methods* **13**, 1036–1042 (2016).
18. A. Wellner *et al.*, *Nat. Chem. Biol.* **17**, 1057–1064 (2021).
19. Z. D. Blount, *eLife* **4**, e05826 (2015).
20. M. M. Poranen *et al.*, *J. Virol.* **80**, 8081–8088 (2006).
21. A. M. Grahn, J. K. Bamford, M. C. O'Neill, D. H. Bamford, *J. Bacteriol.* **176**, 3062–3068 (1994).
22. H. Savilahti, D. H. Bamford, *J. Virol.* **67**, 4696–4703 (1993).
23. K. C. Murphy, *J. Bacteriol.* **173**, 5808–5821 (1991).
24. S. K. Yoo, J. Ito, *J. Mol. Biol.* **218**, 779–789 (1991).
25. P. L. Foster, *Methods Enzymol.* **409**, 195–213 (2006).
26. B. M. Hall, C. X. Ma, P. Liang, K. K. Singh, *Bioinformatics* **25**, 1564–1565 (2009).
27. A. H. Badran, D. R. Liu, *Nat. Commun.* **6**, 8425 (2015).
28. J. Jee *et al.*, *Nature* **534**, 693–696 (2016).
29. H. Lee, E. Popodi, H. Tang, P. L. Foster, *Proc. Natl. Acad. Sci. U.S.A.* **109**, E2774–E2783 (2012).

30. S. H. Joshi, C. Yong, A. Gyorgy, *Nat. Commun.* **13**, 6691 (2022).
31. M. V. Rouches, Y. Xu, L. B. G. Cortes, G. Lambert, *Nat. Commun.* **13**, 3908 (2022).
32. R. Tian *et al*., Code for: Establishing a synthetic orthogonal replication system enables accelerated evolution in *E. coli*, version 1, Zenodo (2023); https://doi.org/10.5281/zenodo.10213374.

ACKNOWLEDGMENTS

We thank the FACS facility at the Medical Research Council Laboratory of Molecular Biology (MRC-LMB), especially P. A. Penttilä, Y. Li, F. Zhang, and D. Nolan, for support. **Funding:** This work was supported by the MRC (grants MC_U105181009 and MC_UP_A024_1008 to J.W.C.). D.C. and Y.G. were supported by European Molecular Biology Organization (EMBO) postdoctoral fellowships (ALTF 715-2022 to D.C. and ALTF 93-2023 to Y.G.). F.B.H.R. was supported by a UK Research and Innovation (UKRI) Marie Skłodowska-Curie Actions (MSCA) guarantee fellowship (EP/Y014154/1). **Author contributions:** R.T. conceptualized the project. R.T. and J.F.Z. designed approaches to establishing the O-replication system. R.T. established and investigated the stability of the O-replication system, designed and tested the O-replicon copy number control system, characterized all error-prone DNAP mutants, and performed the accelerated continuous evolution of *tetA* and GFP. F.B.H.R. designed the helper plasmid, characterized the minimal origin length, tested multiple distinct O-replicons co-maintenance, and analyzed structures of evolved proteins obtained from the continuous evolution experiments. D.C. provided the predicted structure of the O-DNAP, rationally designed nine O-DNAP mutants, analyzed structures of evolved proteins obtained from the continuous evolution experiments, and performed all flow cytometry experiments. Y.G. analyzed structures of evolved proteins obtained from the continuous evolution experiments and analyzed the Sanger sequencing–based determination mutations. K.C.L. prepared next-generation sequencing (NGS) samples. J.W.C., F.B.H.R., and R.T. wrote the manuscript with input from all authors. J.W.C. supervised the project. **Competing interests:** The MRC has filed a provisional patent application related to this work on which R.T., J.F.Z., F.B.H.R., D.C., Y.G., and J.W.C. are listed as inventors. J.W.C. is the founder of and J.F.Z. is a consultant for Constructive Bio. K.C.L. declares no competing interests. **Data and materials availability:** All data are available in the main text or supplementary materials. The computer code to analyze NGS data are available from Zenodo (*32*). The authors agree to provide any materials and strains used in this study upon request.

SUPPLEMENTARY MATERIALS

science.org/doi/10.1126/science.adk1281
Materials and Methods
Figs. S1 to S22
References (*33*–*40*)
Data S1 to S3
MDAR Reproducibility Checklist

Submitted 3 August 2023; accepted 28 November 2023
10.1126/science.adk1281